

# Photopolymerization of Diacetylene Lipid Bilayers and Its Application to the Construction of Micropatterned Biomimetic Membranes

Kenichi Morigaki,<sup>\*,†</sup> Tobias Baumgart,<sup>‡</sup> Ulrich Jonas,  
Andreas Offenhäusser,<sup>§</sup> and Wolfgang Knoll

Max-Planck-Institut für Polymerforschung, Ackermannweg 10, 55128 Mainz, Germany

Received December 18, 2001. In Final Form: March 6, 2002

Photopolymerization of diacetylene-containing amphiphiles in substrate-supported bilayers has been studied in connection with the development of a new fabrication strategy of micropatterned biomimetic membrane systems. Two types of amphiphilic diacetylene molecules were compared, one being a monoalkyl phosphate, phosphoric acid monohexacosyl-10,12-diynyl ester (**1**), and the other being a phospholipid, 1,2-bis(10,12-tricosadiynoyl)-*sn*-glycero-3-phosphocholine (**2**). The bilayers of monomeric diacetylene amphiphiles were deposited onto substrates by the Langmuir–Blodgett/Langmuir–Schaefer methods. Both amphiphiles could be polymerized successfully on oxide and polymer-coated substrates. However, the phospholipid (**2**) showed a markedly higher mechanical stability of the polymerized bilayer films compared with the monoalkyl phosphate (**1**). Micropatterns were imposed in the bilayers by using a physical mask to protect the monomeric lipids partially upon UV irradiation. In the case of **2**, monomeric bilayers could be removed selectively by ethanol after the lithographic photopolymerization, resulting in the formation of wells between the polymerized bilayers. These wells were filled with fluid phosphatidylcholine bilayers by fusion of vesicles. The rigid polymeric bilayer and the fluid biomimetic bilayer could be integrated as a composite bilayer membrane with defined spatial patterns, offering new possibilities to construct complex and versatile biomimetic membrane systems.

## 1. Introduction

Substrate-supported planar lipid bilayers (abbreviated as SPBs in the following) represent a unique type of biomimetic membrane system, where a single lipid bilayer is attached to a solid surface either by physical interactions or by chemical bonds. SPBs are generally designed such that the bilayer membrane mimics some key physical and chemical properties of the biological membrane (e.g., lipid composition, fluidity, resistance to nonspecific protein adsorption, etc.).<sup>1–4</sup> Such artificial membrane systems provide attractive tools both for biophysical studies and for biomedical/environmental applications.<sup>2,3</sup> For example, attempts have been made to integrate membrane proteins in their active form in order to monitor their activities and develop sensor/diagnostic applications based on specific ligand/receptor bindings.<sup>5</sup>

Compared with other formats of artificial membrane systems (lipid vesicles, black lipid membranes, etc.), SPBs possess the unique feature that they can potentially be created in micropatterned geometries, in analogy to the integrated circuit on a silicon wafer. The patterning of SPBs has been reported by using several approaches including the modification of solid substrates and the

microcontact printing technique.<sup>6–11</sup> We have recently reported a novel method for the micropatterning of SPBs based on the lithographic photopolymerization of a diacetylene phospholipid within bilayers.<sup>12</sup> Photopolymerization cross-linked lipid molecules selectively where UV light was irradiated, and the nonirradiated bilayer membranes, which consisted of monomers, could be removed by an organic solvent or by a detergent solution. The resulting wells between polymeric bilayers could be filled with phospholipid bilayers that possess lateral fluidity. The polymeric bilayers acted as a template to incorporate new biomimetic lipid bilayer membranes in a spatially defined manner.

Polymerization of lipidic molecules in lyotropic, self-assembled aggregations (lamellar, cubic, inverted hexagonal, etc.) has attracted considerable attention in the last several decades.<sup>13–15</sup> In particular, stabilization of lipid vesicles (liposomes) by polymerization of lipids has been studied extensively in connection with the potential application for encapsulation of medicinal materials (drug

<sup>†</sup> Current address: National Institute of Advanced Industrial Science and Technology, Ikeda 563-8577, Japan. Fax: +81-727-51-9628. E-mail: morigaki-kenichi@aist.go.jp.

<sup>‡</sup> Current address: School of Applied and Engineering Physics, Cornell University, Clark Hall, Ithaca, NY 14853.

<sup>§</sup> Current address: Institute for Thin Films & Interfaces, Forschungszentrum Jülich, 52425 Jülich, Germany.

(1) Chapman, D. *Langmuir* **1993**, *9*, 39–45.

(2) Sackmann, E. *Science (Washington, D.C.)* **1996**, *271*, 43–48.

(3) Plant, A. *Langmuir* **1999**, *15*, 5128–5135.

(4) Wisniewski, N.; Reichert, M. *Colloids Surf., B* **2000**, *18*, 197–219.

(5) Heyse, S.; Ernst, O. P.; Dienes, Z.; Hofmann, K. P.; Vogel, H. *Biochemistry* **1998**, *37*, 507–522.

(6) Groves, J. T.; Ulman, N.; Boxer, S. G. *Science (Washington, D.C.)* **1997**, *275*, 651–653.

(7) Wiegand, G.; Jaworek, T.; Wegner, G.; Sackmann, E. *Langmuir* **1997**, *13*, 3563–3569.

(8) Jenkins, A. T. A.; Boden, N.; Bushby, R. J.; Evans, S. D.; Knowles, P. F.; Miles, R. E.; Ogier, S. D.; Schönherr, H.; Vancso, G. J. *J. Am. Chem. Soc.* **1999**, *121*, 5274–5280.

(9) Hovis, J. S.; Boxer, S. G. *Langmuir* **2000**, *16*, 894–897.

(10) Cremer, P. S.; Yang, T. *J. Am. Chem. Soc.* **1999**, *121*, 8130–8131.

(11) Groves, J. T.; Mahal, L. K.; Bertozzi, C. R. *Langmuir* **2001**, *17*, 5129–5133.

(12) Morigaki, K.; Baumgart, T.; Offenhäusser, A.; Knoll, W. *Angew. Chem., Int. Ed. Engl.* **2001**, *40*, 172–174.

(13) Ringsdorf, H.; Schlarb, B.; Venzmer, J. *Angew. Chem., Int. Ed. Engl.* **1988**, *27*, 113–158.

(14) Singh, A.; Schnur, J. M. In *Phospholipids Handbook*; Cevc, G., Ed.; Marcel Dekker: New York, 1993.

(15) O'Brien, D. F.; Armitage, B.; Benedicto, A.; Bennett, D. E.; Lamparski, H. G.; Lee, Y. S.; Srisiri, W.; Sisson, T. M. *Acc. Chem. Res.* **1998**, *31*, 861–868.

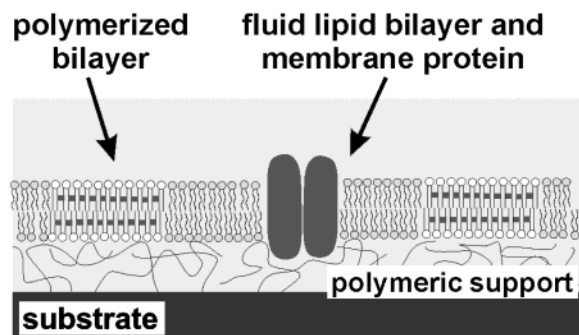


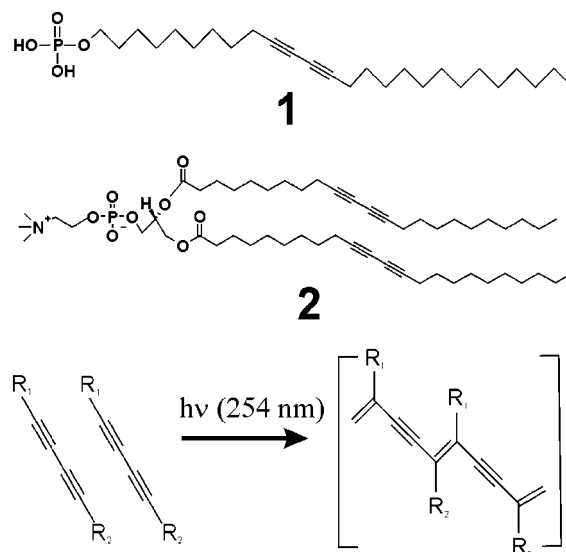
**Figure 1.** Schematic illustration of a substrate-supported biomimetic membrane that consists of patterned polymeric lipid bilayers and fluid lipid bilayers supported by a polymeric spacer layer.

delivery).<sup>16</sup> Lipid molecules having various moieties (e.g., dienoyl, sorbyl, diacetylene, etc.) were synthesized and polymerized in situ within the bilayers. Upon polymerization, the bilayers became significantly less soluble in organic solvents or detergent solutions.<sup>17–20</sup> In addition, decrease in the lateral diffusion constant and the permeation coefficient of the bilayers was observed.<sup>21,22</sup>

Micropatterning of SPBs by lithographic photopolymerization of lipid bilayers aims to achieve both spatial control and stabilization of biomimetic membranes. One distinctive feature of this approach in comparison with previously reported micropatterning methods is the fact that the pattern is imprinted in the bilayer membrane. It enables the patterned two-dimensional structure to be separated from the substrate by a thin polymeric layer, which is often necessary for the successful incorporation of membrane proteins into SPBs.<sup>23–27</sup> An envisioned membrane structure is depicted in Figure 1. Integrated membrane systems with defined spatial patterns should enable the reproduction of various complex biological signal transduction events in an artificial platform. Nevertheless, there are various technical challenges to be addressed to create such complex structures in a controlled way.

Herein we report on the photopolymerization process of diacetylene lipid bilayers on solid surfaces. We have compared the photopolymerization behaviors of two diacetylene-containing amphiphiles, a monoalkyl phosphate (**1**) and a phospholipid (**2**) (Scheme 1) on oxide and polymer-coated substrates. The choice of the diacetylene group for studying polymerization of bilayers was based on the following two properties. (i) Poly(diacetylenes) form long conjugation of ene–yne backbones that absorb UV/visible light strongly. Furthermore, certain types of poly(diacety-

**Scheme 1.** Chemical Structures of Diacetylene-Containing Monoalkyl Phosphate (**1**) and Phospholipid (**2**) and Their Photopolymerization Scheme



lenes) show a marked fluorescence. These properties facilitate the characterization of the polymers both spectroscopically and microscopically. (ii) Diacetylene molecules polymerize only in a highly ordered state (i.e., topochemical or solid-state polymerization),<sup>28,29</sup> and the polymerization is very sensitive to the factors that affect the molecular packing.<sup>30–32</sup> In the case of SPBs, the molecular packing within the bilayer is influenced by the substrate.<sup>33,34</sup> Both **1** and **2** showed distinctive polymerization behaviors, depending on the type of substrate. The comparison of two different types of amphiphiles, one being a single alkyl chain lipid and the other being a phospholipid with two alkyl chains, yielded valuable insight into some important aspects for the development of patterned biomimetic membranes based on the lithographic photopolymerization of bilayers. The single chain amphiphile **1** showed a markedly higher reactivity compared with the phospholipid **2**. The conjugation of the ene–yne backbones was also longer in polymerized **1** bilayers accordingly and showed distinctive spectral features (mixtures of the blue and red polymers) depending on the underlying substrates. Therefore, bilayers of **1** provided a convenient system to systematically study the influence of the substrate materials on the photopolymerization. The phospholipid **2**, on the other hand, proved to be a suitable material for the purpose of the micropatterning of SPBs due to the high stability of polymerized bilayers. The comparison of stability between polymerized **1** and **2** suggested the importance of cross-links within the polymeric backbones (only possible with **2**) for the stabilization of the bilayer membranes.

(16) Freeman, F. J.; Chapman, D. In *Liposomes as drug carriers*; Gregoriadis, G., Ed.; John Wiley & Sons: New York, 1988; pp 821–839.

(17) Johnston, D. S.; McLean, L. R.; Whittam, M. A.; Clark, A. D.; Chapman, D. *Biochemistry* **1983**, *22*, 3194–3202.

(18) Leaver, J.; Alonso, A.; Durrani, A. A.; Chapman, D. *Biochim. Biophys. Acta* **1983**, *732*, 210–218.

(19) Takeoka, S.; Ohgushi, T.; Tsuchida, E. *Macromolecules* **1995**, *28*, 7660–7666.

(20) Sisson, T. M.; Lamparski, H. G.; Kölschens, S.; Elayadi, A.; O'Brien, D. F. *Macromolecules* **1996**, *29*, 8321–8329.

(21) Sackmann, E.; Eggl, P.; Fahn, C.; Bader, H.; Ringsdorf, H.; Schollmeier, M. *Ber. Bunsen-Ges. Phys. Chem.* **1985**, *89*, 1198–1208.

(22) Kölschens, S.; Lamparski, H.; O'Brien, D. F. *Macromolecules* **1993**, *26*, 398–400.

(23) Spinke, J.; Yang, J.; Wolf, H.; Liley, M.; Ringsdorf, H.; Knoll, W. *Biophys. J.* **1992**, *63*, 1667–1671.

(24) Wong, J. Y.; Majewski, J.; Seitz, M.; Park, C. K.; Israelachvili, J.; Smith, G. S. *Biophys. J.* **1999**, *77*, 1445–1457.

(25) Wong, J. Y.; Park, C. K.; Seitz, M.; Israelachvili, J. *Biophys. J.* **1999**, *77*, 1458–1468.

(26) Wagner, M. L.; Tamm, L. K. *Biophys. J.* **2000**, *79*, 1400–1414.

(27) Sackmann, E.; Tanaka, M. *TIBTECH* **2000**, *18*, 59–64.

(28) Bloor, D.; Chance, R. R., Eds. *Polydiacetylenes. Synthesis, Structure and Electronic Properties*; Martinus Nijhoff Publishers: Dordrecht/Boston/Lancaster, 1985.

(29) Cantow, H.-J., Ed. *Polydiacetylenes*; Springer-Verlag: Berlin, 1984.

(30) Charych, D. H.; Nagy, J. O.; Spevak, W.; Bednarski, M. D. *Science (Washington, D.C.)* **1993**, *261*, 585–588.

(31) Jonas, U.; Shah, K.; Norvez, S.; Charych, D. H. *J. Am. Chem. Soc.* **1999**, *121*, 4580–4588.

(32) Okada, S.; Peng, S.; Spevak, W.; Charych, D. *Acc. Chem. Res.* **1998**, *31*, 229–239.

(33) Kuriyama, K.; Kikuchi, H.; Kajiyama, T. *Langmuir* **1996**, *12*, 2283–2288.

(34) Britt, D. W.; Hofmann, U. G.; Möbius, D.; Hell, S. W. *Langmuir* **2001**, *17*, 3757–3765.

## 2. Materials and Methods

**2.1. Materials.** Diacetylene-containing monoalkyl phosphate, phosphoric acid monohexadecanoic-10,12-diynyl ester (**1**), was a gift from Professor Helmut Ringsdorf. Diacetylene phospholipid, (1,2-bis(10,12-tricosadiynoyl)-*sn*-glycero-3-phosphocholine) (**2**) and phosphatidylcholine from egg yolk (egg-PC) were purchased from Avanti Polar Lipids (Alabaster, AL). NBD-PE (*N*-(7-nitrobenz-2-oxa-1,3-diazol-4-yl)-1,2-dihexadecanoyl-*sn*-glycero-3-phosphoethanolamine) was purchased from Molecular Probes (Eugene, OR). Chitosan ( $M_w$  600 000), polyethylimine (PEI;  $M_w$  2000), and sodium dodecyl sulfate (SDS) were from Fluka (Buchs, Switzerland). Other chemicals were purchased from Sigma (St. Louis, MO). All the commercially obtained chemicals were used without further purification. As the substrates of SPB, we have used either slide glass (Menzel, Braunschweig, Germany), polished quartz (Hellma, Mühlheim, Germany), or thermally oxidized silicon (oxide layer thickness 154–163 nm, IMM, Mainz, Germany).

**2.2. Substrate Cleaning and Modification with Polymers.** The substrates were cleaned first with a commercial detergent solution (0.5% Hellmanex/water, Hellma, Mühlheim, Germany), rinsed with deionized water, treated in a warm concentrated sulfuric acid (70 °C for 15 min), rinsed with deionized water extensively, and then dried in a vacuum oven at 110 °C. This protocol resulted in sufficiently clean and hydrophilic surfaces for the adsorption of polymers and lipid bilayer membranes. Chitosan and PEI were adsorbed onto the substrates from dilute aqueous solutions (ca. 1 w/w %). In the case of chitosan, a dilute acetic acid solution (1 v/v %) was used to dissolve the polymer in a slightly acidic solution. The nonadsorbed polymers were removed from the substrate surfaces by extensive rinsing with the acetic acid solution and deionized water. The thickness of the adsorbed polymer layer was measured by ellipsometry for the dry films to be ca. 1 nm for chitosan and ca. 6 nm for PEI.

**2.3. Preparation of Supported Planar Bilayers.** Bilayers of monomeric **1** and **2** were deposited onto solid substrates from the air/water interface by the Langmuir–Blodgett (LB) and Langmuir–Schaefer (LS) methods using a KSV5000 Langmuir trough (KSV Instruments, Helsinki, Finland).<sup>35</sup> Molecules of **1** and **2** were spread from dichloromethane/methanol (9:1 v/v) and chloroform solutions, respectively. The lipids formed stable monolayers at the air/water interface up to a surface pressure of 40 mN/m at 20 °C. The monolayers were transferred onto solid substrates at 35 mN/m (fully condensed state). The first monolayer was deposited by dipping and withdrawing the substrate vertically (LB method). The second monolayer was deposited onto the hydrophobic surface of the first monolayer by pressing the substrate horizontally through the monolayer at the air/water interface and dropping it into the subphase (LS method). The transferred film area corresponded well to the theoretical values for both the LB and LS procedures, indicating that bilayers were built on both oxide and polymeric substrates used. The bilayer structure is also supported by atomic force microscopy measurements. The samples were collected from the trough and stored in deionized water (in the dark) for the photopolymerization.

**2.4. Photopolymerization of Bilayers.** As the light source, we used either a small low-pressure mercury lamp (2 W, UVP, Pen-Ray, Upland, CA) or a cross-linker (40 W, UVP CL-1000, Upland, CA) that emit strong UV light at 254 nm. **1** could be polymerized in water in the presence of oxygen. In the case of **2**, oxygen had to be removed from the aqueous solution prior to photopolymerization, since presence of oxygen inhibited the polymerization, presumably by quenching diacetylene radicals.<sup>36</sup> The polymerization was conducted in a closed system that comprised a water reservoir, a pump, and a cell (ca. 4 mL volume). The water reservoir was depleted from oxygen by purging with

argon. Oxygen-free water was circulated continuously by the pump (3.8 mL/min) through the cell where the polymerization of the bilayers was conducted. The cell had two walls in the opposite sides, one being the sample (SPB was inside the cell) and the other being a quartz window through which UV light was illuminated. The desired patterns were transferred to the SPB in the photopolymerization process by illuminating the sample through a mask (a quartz slide with a patterned gold coating), which was put over the SPB (separated by a thin water layer) inside the cell. After sufficient circulation of deaerated water (typically 15 min), the pump was stopped and the photopolymerization was started. The distance between the UV light source and the SPB was 5 and 20 cm for the Pen-Ray lamp and the cross-linker, respectively.

**2.5. Incorporation of Fluid Bilayers into the Wells between Polymerized Bilayers.** To remove unreacted monomers, the samples were immersed either in a detergent solution (80 mM SDS) or in ethanol for 10 min and rinsed extensively with deionized water. For the incorporation of new lipid bilayers into the lipid-free wells, the vesicle fusion method was applied.<sup>37</sup> Vesicle suspensions of egg-PC containing 1 mol % NBD-PE (1 mM in a 0.05 M phosphate buffer with 0.1 M NaCl (pH 7.0)) were extruded through a filter with pores of diameter 50 nm (Nuclepore, Corning, Acton, MA) by using an extruder (LiposoFast, Avestin, Ottawa, Canada). A 100–200  $\mu$ L portion of the filtrate was placed onto the patterned **2** bilayer samples and sandwiched with another slide glass using a thin cover glass as a spacer in order to avoid scratching the patterned SPB surfaces. The samples were rinsed with a 0.05 M phosphate buffer solution (pH 7.0, containing 0.1 M NaCl) after 5 min.

**2.6. UV–vis Absorption and Fluorescence Spectroscopy.** UV–vis absorption spectra were obtained by using a Perkin-Elmer  $\lambda$ 9 spectrophotometer (Perkin-Elmer Analytical Instruments, Shelton, CT). Fluorescence spectra were obtained with a SPEX F212 (Jobin-Yvon, Edison, NJ) by using the front-face mode (the sample was placed at an angle of 45° from the excitation light incidence and the fluorescence was measured at 22.5°). For the fluorescence measurements of SPB, the samples were dried by nitrogen before the measurements.<sup>38</sup> This procedure did not affect the fluorescence spectra of the poly(diacetylene) films (the obtained spectra were identical with the in situ measurements).

**2.7. Microscopy Observation.** Differential interference contrast images were taken with an Axioskop microscope (Carl Zeiss, Göttingen, Germany) equipped with epi-illumination (HBO 50 lamp) and a color CCTV camera WL-CL 700/G (Panasonic, Osaka, Japan). For fluorescence microscopy, an invertoscope (IX-70, Olympus, Tokyo, Japan) equipped with a mercury lamp (HBO-100, Olympus) was used. The excitation and observation wavelength were 488 and 530 nm, respectively. Fluorescence microscopy images were obtained with a light-enhancing camera (Extended ISIS: Photonic Sciences, Robertsbridge, UK) and a frame grabber card (AG-5: Scion, Frederick, MD) and were processed using softwares Scion Image (Scion, Frederick, MD) or Image Pro Plus (Media Cybernetics, Leiden, Netherlands).

## 3. Results and Discussion

**3.1. Absorption/Fluorescence Spectra of Polymerized **1** in Suspended Bilayers.** In the current study we have exploited fluorescence excitation spectroscopy extensively in order to detect and characterize the in situ polymerization. Fluorescence spectroscopy turned out to be highly convenient for reflective substrates such as oxidized silicon, where direct measurement of absorption spectra is difficult due to the optical interference. We describe first the absorption and fluorescence spectra of polymerized **1** in suspended bilayers (vesicles) as a

(35) Another potential approach for the generation of adsorbed planar bilayer membranes, the vesicle fusion process, failed for these lipids, due to the high melting temperatures of the bilayers. At ambient temperature the bilayers were in the solidlike state. Even at elevated temperatures the attempts for vesicle fusion failed, presumably because of the stiffness of bilayers.

(36) Day, D.; Ringsdorf, H. *J. Polym. Sci., Polym. Lett. Ed.* **1978**, *16*, 205–210.

(37) Brian, A. A.; McConnell, H. M. *Proc. Natl. Acad. Sci. U.S.A.* **1984**, *81*, 6159–6163.

(38) This protocol was employed in order to minimize the effect of contamination. Since we characterized the polymerization of single bilayers by fluorescence spectroscopy, signals from foreign fluorophores (contaminants from the lab environment) often overwhelmed that of the samples and made reproducible measurements difficult. Foreign contaminants could diffuse onto the sample surfaces especially easily when we worked with wet samples.



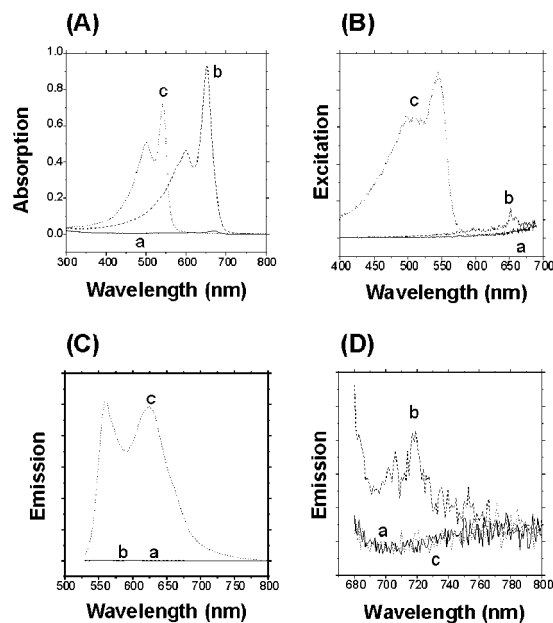


**Figure 2.** Absorption and fluorescence spectra of **1** vesicle suspensions (0.05 mM of **1** in water) were measured for (a) monomer, (b) blue polymer formed by UV irradiation (Pen-Ray, 2 min), and (c) red polymer formed by heating the blue polymer: (A) absorption spectra (0.05 mM, optical path length = 1 cm); (B) fluorescence excitation spectra (emission was measured at 720 nm); (C) fluorescence emission spectra (excitation at 500 nm); (D) fluorescence emission spectra (excitation at 650 nm).

reference for further spectroscopic analysis of SPB (Figure 2). Vesicle suspensions of **1** were prepared by dispersing the lipid molecules in water by probe sonication. Monomeric bilayers of **1** showed no absorption/fluorescence between 300 and 800 nm ((a) in Figure 2), and the sample solution was transparent. The vesicle suspensions became dark blue upon UV irradiation due to the formation of polymers that had strong absorption bands between 600 and 700 nm (blue polymer, (b) in Figure 2A). When the sample was heated, the polymeric bilayers underwent a structural transition and the absorption bands shifted toward shorter wavelengths (450–550 nm, (c) in Figure 2A). The color of the suspensions changed to pink or red accordingly (red polymer). This chromatic transition is known from literature as a consequence of the conformational relaxation of the polymer backbone and shortening of the effective conjugation length.<sup>39</sup> Figure 2B compares the fluorescence excitation spectra that were obtained for the same vesicle suspensions by measuring the fluorescence emission intensity at 720 nm as a function of the excitation light wavelength. Whereas the red polymer had strong excitation bands between 425 and 575 nm (c) that roughly corresponded to its absorption bands, the blue polymer showed only a very weak excitation band between 600 and 700 nm (b). This observation also agrees with previous reports where the fluorescence was mainly observed from the red polymers.<sup>40–43</sup> The fluorescence from the blue polymer is reduced, at least in part, due to increased radiationless

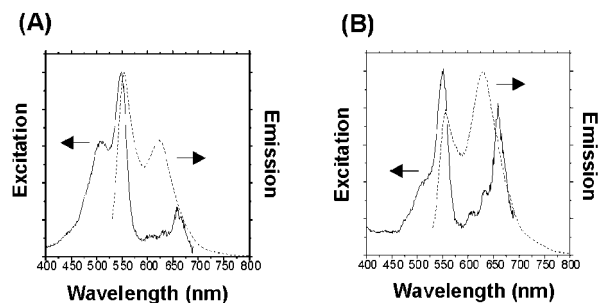


**Figure 3.** Fluorescence spectra of **1** bilayers polymerized on (A) quartz and (B) oxidized silicon substrates (UV irradiation, cross-linker, 400 mJ). The excitation spectra (solid lines) were obtained by measuring the emission at 720 nm. The emission spectra (dashed lines) were obtained by the excitation at 500 nm.

deactivation processes.<sup>41</sup> Emission spectra from the blue and red polymers have been also measured (Figure 2C,D, excitation at 500 nm for (C) and 650 nm for (D), respectively). Fluorescence was indeed observed to arise from specific bands that corresponded to the red polymer ((c) in Figure 2C) and the blue polymer ((b) in Figure 2D).<sup>44</sup> The absorption and fluorescence spectra of suspended **1** bilayers are in good agreement with the reported spectroscopic observations.

**3.2. Photopolymerization of 1 in SPB.** Now we turn to the polymerization of the diacetylene amphiphiles in SPB adsorbed on various substrates. Figure 3 compares the fluorescence spectra of polymerized **1** on quartz and oxidized silicon substrates. The obtained excitation spectra (solid lines in Figure 3) were considerably different from the vesicle samples (see Figure 2B) and showed strong dependency on the type of substrates. The excitation band between 600 and 700 nm that should arise from the blue polymer was significantly enhanced in the case of oxidized silicon substrates (Figure 3B). As in the case of vesicles, the blue polymer could be transformed into the red polymer by treatment with heat or organic solvents. Figure 4 shows the changes in absorption and fluorescence excitation spectra that were induced by immersing the polymeric bilayers in ethanol. The spectral bands between 600 and 700 nm disappeared after the ethanol treatment, whereas the spectral bands at shorter wavelength retained the identical shape.<sup>45</sup> It becomes clear from this result that the initially formed polymeric bilayers contained both the red and blue forms. Upon treatment with ethanol they are converted into a purely red state due to solvent-induced conformational changes in the polymer backbones. It is currently not clear how the two types of polymers coexist. They may be spatially resolved or molecularly mixed. It has been reported that red polymers are found at the rim of the blue polymer domains in Langmuir–Blodgett films.<sup>46</sup> The distinctive spectral features on various substrates were reproducible and indicated different polymerization states. The different behaviors between quartz and oxidized silicon are rather surprising, since both materials should have similar chemical compositions. However, the difference persisted regardless of the surface cleaning methods for these substrates. Oxidized silicon substrates had slightly less hydrophilic surfaces compared

(39) Huo, Q.; Russell, K. C.; Leblanc, R. M. *Langmuir* **1999**, *15*, 3972–3980.

(40) Olmsted, J., III; Strand, M. *J. Phys. Chem.* **1983**, *87*, 4790–4792.

(41) Warta, R.; Sixl, H. *J. Chem. Phys.* **1988**, *88*, 95–99.

(42) Carpick, R. W.; Mayer, T. M.; Sasaki, D. Y.; Burns, A. R. *Langmuir* **2000**, *16*, 4639–4647.

(43) Carpick, R. W.; Sasaki, D. Y.; Burns, A. R. *Langmuir* **2000**, *16*, 1270–1278.

(44) The fluorescence from the blue polymer was much weaker compared with that of the red polymer, as the low signal-to-noise ratio of line b in Figure 2D indicates.

(45) The spectra were normalized, so that the spectral shapes could be compared. The bands for the red polymer after the ethanol treatment were generally stronger than those of the blue polymer.

(46) Bubeck, C.; Tieke, B.; Wegner, G. *Ber. Bunsen-Ges. Phys. Chem.* **1982**, *86*, 495–498.

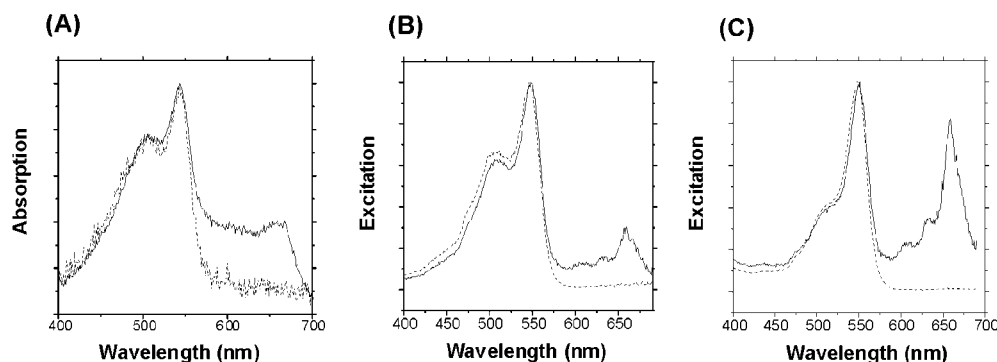


**Figure 4.** Spectral changes in polymeric **1** bilayers induced by ethanol treatment: (A) absorption spectra of a single bilayer on a quartz substrate; (B) fluorescence excitation spectra (emission at 720 nm) on a quartz substrate (the same sample as (A)); (C) fluorescence excitation spectra (emission at 720 nm) on an oxidized silicon substrate; solid lines, UV polymerized bilayers before the ethanol treatment; dashed lines, after the ethanol treatment.

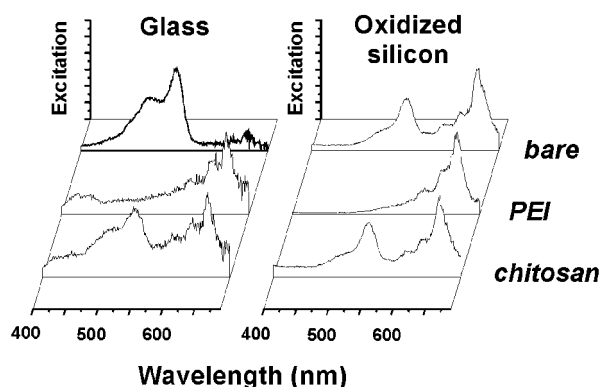


**Figure 5.** Fluorescence excitation spectra of polymerized **1** bilayers were compared on glass and oxidized silicon substrates that were modified with either PEI or chitosan (UV irradiation, cross-linker, 400 mJ). The emission was measured at 720 nm.

with quartz and glass substrates.<sup>47</sup> This might have affected the molecular alignment of **1** bilayers. We observed for microscope slide glass substrates very similar polymerization behaviors as quartz substrates (see below).

The surface-dependent nature of the polymerization was more evident when we modified the substrate surface with thin polymer layers. As the supporting polymeric material two water soluble polyelectrolytes, PEI and chitosan, were used. Both polymers become positively charged by protonation at low pH (<6) and adsorb strongly onto negatively charged substrates (glass and oxidized silicon) from the aqueous phase by electrostatic interactions. A thin polymeric layer remains on the substrate after extensive rinse with water. Bilayers of **1** were deposited onto the polymeric supports by the LB/LS techniques, and they were subsequently polymerized by UV light. The obtained fluorescence excitation spectra are compared in Figure 5. The excitation spectra of polymerized **1** on bare substrates showed distinctive spectral patterns on glass and oxidized silicon substrates. A strong excitation band between 600 and 700 nm was observed for the oxidized silicon substrate, as described above. The polymerized **1** on glass, on the other hand, showed strong excitation bands between 425 and 575 nm, and those between 600 and 700 nm were relatively weak.<sup>48</sup> This spectral feature is similar to the polymerization on quartz (see Figure 3). When we used polyelectrolyte-modified glass or silicon as the

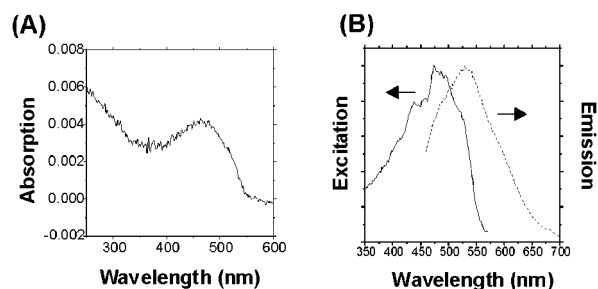


**Figure 6.** Absorption and fluorescence spectra of a polymeric **2** bilayer on a quartz substrate: (A) absorption spectrum (UV irradiation, Pen-Ray, 9 min); (B) fluorescence excitation/emission spectra (UV irradiation, Pen-Ray, 30 min). The excitation spectrum (solid line) was obtained by measuring the emission at 600 nm. The emission spectrum (dashed line) was obtained by the excitation at 430 nm.

substrates, however, the excitation spectra were changed considerably. Polymerized **1** bilayers on PEI showed only the excitation bands between 600 and 700 nm, indicating the formation of blue polymers. In contrast, chitosan substrates resulted in the formation of a mixture of the red polymers and the blue polymers (both spectral bands between 425 and 575 nm and between 600 and 700 nm were observed). These spectra were obtained regardless of the underlying substrate material (glass or oxidized silicon), indicating that the polymerization of **1** bilayers was determined by the type of the polymer (PEI or chitosan). Although the polymeric underlayers are very thin, they apparently determine the surface properties of the substrates and direct the polymerization process of the bilayers.<sup>49</sup>

**3.3. Photopolymerization of 2 in SPB.** The bilayers of **2** were much less photoreactive compared with **1** bilayers. **2** polymerized only in an oxygen-free atmosphere at much longer UV irradiation, whereas **1** polymerized rapidly in ambient atmosphere. The higher reactivity of **1** is presumably due to the ability of the single chain amphiphiles to pack in ordered crystalline bilayer structures. In the case of **2**, the glycerol group of the phospholipid imposes sterical restrictions to the packing of the two alkyl chains bearing the diacetylene moieties.<sup>50</sup> The attenuated polymerization of **2** apparently resulted in a shorter conjugation length compared with **1** bilayers as seen in the absorption spectra (Figure 6A). When the

(47) Both quartz and oxidized silicon surfaces had contact angles that were close to zero. However, we noted slightly different wettability as we observed the drying behavior of water droplets on the substrates.

(48) The fluorescence spectra of **1** bilayers on glass substrates had a larger noise because of the autofluorescence from glass that was subtracted from the sample spectra.

(49) These results also indicate that the reflectivity of silicon substrates did not cause the different polymerization behaviors of **1** bilayers on oxidized silicon substrates with respect to the bilayers on quartz/glass substrates.

(50) Lopez, E.; O'Brien, D. F.; Whitesides, T. H. *J. Am. Chem. Soc.* **1982**, *104*, 305–307.

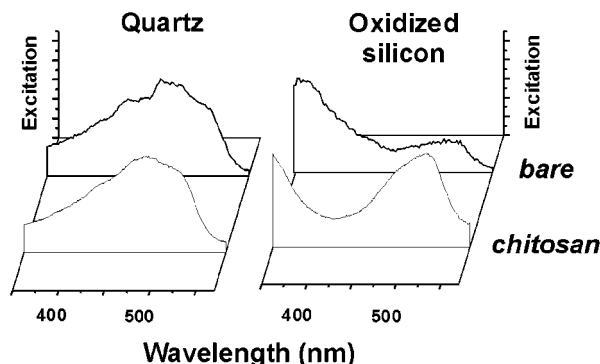


**Figure 7.** Fluorescence excitation spectra of polymerized **2** bilayers were compared on quartz and oxidized silicon substrates that were modified with a thin layer of chitosan (UV irradiation, Pen-Ray, 20 min). The emission was measured at 600 nm.

bilayer was polymerized on quartz, the absorption maximum was observed around 470 nm. The conjugated diacetylene polymer of **2** also emitted strong fluorescence, as shown in Figure 6B. The shape of excitation spectrum corresponds roughly to the absorption spectrum. The polymerization on oxidized silicon resulted in an even shorter conjugation length (the excitation was observed predominantly below 400 nm, see Figure 7).

Polymerization of **2** bilayers was also studied on a thin polymer layer (chitosan) that was adsorbed on quartz and oxidized silicon substrates. The fluorescence excitation spectra are shown in Figure 7. In the case of quartz substrates, the polymerization on the chitosan support occurred in the same way as the case of bare substrates. However, the presence of chitosan support had a more significant effect for oxidized silicon substrates. The excitation band between 450 and 550 nm was enhanced when the substrate was modified by the chitosan support. The bilayer on chitosan contained apparently a larger fraction of the polydiacetylene species with a longer conjugation length. These results show that the polymerization behavior of bilayers **2** is also strongly affected by the presence of a polymeric support layer.

**3.4. Lithographic Photopolymerization of the Bilayers and Its Application to the Construction of Micropatterned Biomimetic Membranes.** By protecting the monomeric bilayer selectively with a mask upon UV light exposure, we could create patterns of polymeric bilayer domains. A differential interference contrast microscope image of the patterned **1** bilayer is shown in Figure 8. The fine texture with the bright granules observed in the polymerized areas corresponds to crystalline domains of polymeric **1**. This texture was also found in the fluorescence microscopy.<sup>51</sup> The polymeric bilayers of **1** were mechanically unstable and peeled off easily from the substrate when the samples were rinsed in water.

Figure 9A shows fluorescence micrographs of patterned **2** bilayers. The polymerized areas are bright due to fluorescence from the conjugated polydiacetylene backbones. Polymerized bilayers of **2** appeared more homogeneous compared with those from **1** presumably due to smaller crystalline domains. Furthermore, the polymerized bilayers were mechanically stable and the material remained even after treatments with organic solvents and detergent solutions. Patterned polymeric bilayers could be created also on chitosan layers (data not shown). To

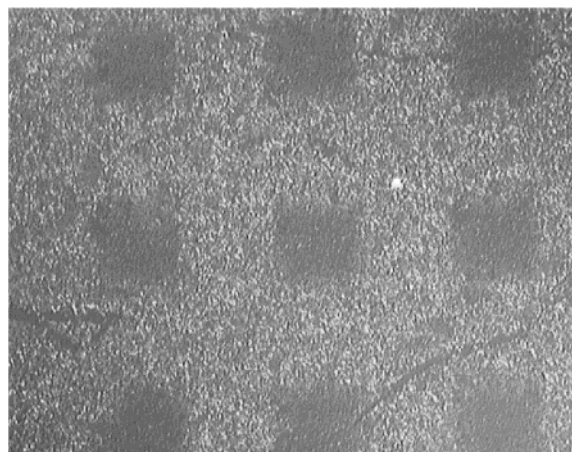


**Figure 8.** Differential interference contrast image of a **1** bilayer that was polymerized with a mask (UV irradiation, cross-linker, 200 mJ). The polymerized bilayer area (grid) surrounds square corrals of monomeric **1** bilayers. The size of the corrals was 50  $\mu\text{m}$ .

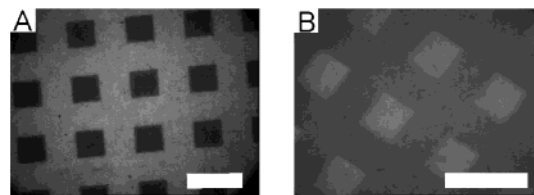


**Figure 9.** Fluorescence microscope images of patterned **2** bilayers on a glass. (A) The brightly fluorescent area (grid) was polymerized by UV irradiation (Pan-Ray, 60 min from 10 cm distance). In the square corrals **2** molecules were protected by the mask and remained monomeric. (B) Monomeric bilayers of **2** were removed with ethanol and lipid bilayers of egg-PC containing 1 mol % NBD-PE were introduced into the same corrals by the vesicle fusion method. The square corrals are brightly fluorescent due to NBD-PE molecules. The scale bars correspond to 100  $\mu\text{m}$ .

understand the different behaviors of polymerized **1** and **2**, we could consider two factors that are potentially related to the stability of polymerized bilayers. First, **2** has two diacetylene moieties in a single molecule. The cross-linked network of polymeric chains formed within the bilayer is expected to make the film mechanically robust.<sup>52</sup> Second, bilayers of **1** apparently have a higher degree of crystallinity compared with **2**, as suggested by its larger crystalline domains and efficient polymerization. This might result in the formation of sharp domain boundaries and packing defects, leading to a lower mechanical stability of the membrane on the substrate.

Stability of polymerized bilayers depended on the duration of the UV light irradiation for photopolymerization, as well. Bilayers of **2** that were polymerized by relatively short irradiation were dissolved by ethanol or SDS solutions and mostly removed from the substrate surface. The polymeric bilayers became resistant toward solubilization, only if the UV irradiation time was sufficiently long.<sup>53</sup> The UV-vis absorption band of the polymerized **2** bilayers at 470 nm grew rapidly upon UV light irradiation, indicating the rapid formation of conjugated polymeric backbones. However, the intensity of this spectral band was not directly correlated to the stability of polymerized bilayers. It is partially because

(51) The boundaries between the polymerized and nonpolymerized parts are unclear in Figure 8. This broadened interface is due to the stray light during the lithographic exposure process rather than propagation of the polymerized domains.

(52) Currently we do not have direct information on the degree of cross-link, since it is not accessible from the spectroscopic data.

(53) In the case of irradiation with a Pen-Ray lamp from a distance of 5 cm, an exposure time of 10 min or longer was necessary to ensure the formation of stable polymeric bilayers.



the effective conjugation length is limited by the local conformations of polymer backbones, and the absorption band does not represent longer polymer chains that might exist in the bilayers. More importantly, the absorption spectra do not give information concerning the degree of cross-linking between the polymer chains. Therefore, although we do not have information on the degree of cross-linking, our interpretation of the observed stability changes by the UV light irradiation time is that the bilayers have longer and more cross-linked polymeric backbones, if one photopolymerizes them for longer time.

Since polymerized **1** bilayers were found to be mechanically unstable, further investigation of patterned bilayers was carried out only with the bilayers of polymerized **2**. After the photopolymerization, unreacted monomers were removed from the bilayer by immersing the samples in ethanol. To incorporate new lipid bilayers into the lipid-free domains, we have fused small unilamellar vesicles (extruded through a filter with pores of diameter ca. 50 nm) of phosphatidylcholine from egg yolk (egg-PC) doped with 1 mol % of the fluorescently labeled lipid NBD-PE. Observation by the fluorescence microscope revealed that the areas where the monomeric bilayers had been removed were refilled with egg-PC bilayers and became intensely fluorescent due to the incorporated NBD-PE (Figure 9B). It should be noted that the polymerized bilayer domains (grid), which are fluorescent in Figure 9A, appear dark in Figure 9B due to the strong fluorescence from the NBD-PE containing bilayers in the corrals. The incorporated egg-PC/NBD-PE bilayers retained the lateral fluidity at room temperature, and the polymerized bilayers acted as a barrier that confined the fluid bilayers. This was proven by the following two sets of experiments. First, NBD-PE molecules in the fluid bilayers were bleached by illuminating an intense light on a selected area of the membrane (the illumination spot diameter was typically ca. 100  $\mu\text{m}$ ). If an egg-PC bilayer was located in a square corral surrounded by polymeric bilayers, bleaching of NBD-PE molecules within the corral resulted in complete loss of fluorescence from the particular corral and no recovery of fluorescence was observed (Figure 10A before, and Figure 10B after bleaching). Illumination of the polydiacetylene bilayer with the same intensity and time did not result in a decrease of fluorescence intensity, showing the high photostability of the polydiacetylene matrix and the absence of NBD-PE in these regions. On the other hand, if the polymeric bilayers were created as parallel lines, the areas between them formed narrow channels of fluid lipid bilayers. In such a geometry, egg-PC and NBD-PE molecules could diffuse through the channels. Therefore, photobleaching of NBD-PE resulted in temporal depression of fluorescence within the illuminated spot and along the connected channel. Parts C and D of Figure 10 illustrate fluorescence gradient created by the photobleaching and diffusion of NBD-PE molecules. In addition to the fluorescence micrograph shown in Figure 10C, a schematic drawing is given in Figure 10D for clarity. Note the gradient of the brightness in Figure 10C (from top right through bottom left) that indicates the concentration gradient of NBD-PE molecules.

The second experiment to visualize the role of polymerized domains as a barrier was the diffusion of negatively charged NBD-PE in an applied electric field. This technique has been used previously to prove the confinement of lipids in defined geometries and to determine their lateral diffusion constants.<sup>54</sup> A horizontal electric field

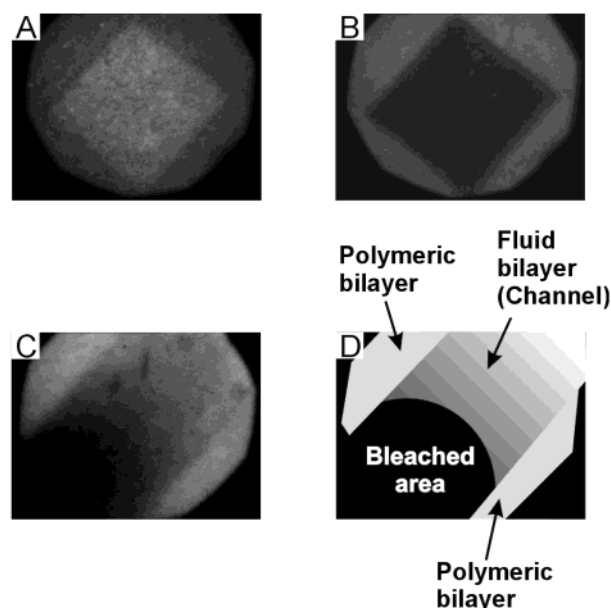


**Figure 10.** Fluorescence micrographs of egg-PC/NBD-PE bilayers incorporated into the wells between polymeric bilayers. A single corral and a channel (size 50  $\mu\text{m}$ ) were bleached by a strong illumination under the microscope objective. In the case of the corral, the fluorescence of NBD-PE was bleached completely (from (A) to (B)), whereas the channel retained the fluorescence partially, because NBD-PE molecules were supplied continuously by diffusion (C). (The molecules at the left bottom side of the channel were bleached and new molecules were supplied from the right upper side (concentration gradient).) (D) Schematic drawing of the image in (C) that depicts the fluid bilayer channel and the concentration gradient of NBD-PE.

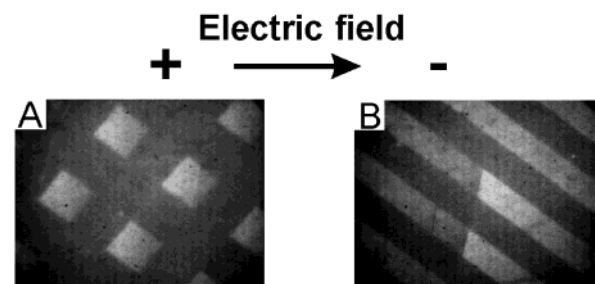


**Figure 11.** Fluorescence micrographs of the patterned bilayers with incorporated egg-PC/NBD-PE bilayers in each corral under the influence of an electric field ( $E$ ) in the direction of the indicated arrow. The negatively charged NBD-PE molecules in the fluid bilayer membranes drifted and formed concentration gradients. The molecules were blocked by barriers of the polymerized bilayer (A) or by a line defect within the channels (B). The size of the corrals and channels (width) was 50  $\mu\text{m}$ .

was applied by using a homemade electrophoresis cell. Under the applied electric field charged lipid molecules (in the current case NBD-PE) diffuse preferentially to one direction and build a concentration gradient (Figure 11). It can be seen in these pictures that NBD-PE molecules are accumulated at the sites where their diffusion is hindered. In Figure 11A, diffusion of NBD-PE was blocked at the left side of the corrals (the boundaries between the fluid and polymerized membrane domains). On the other hand, the diffusion of NBD-PE can be seen in Figure 11B along two channels that were partially blocked by a line defect across the channels. These results strongly indicate that the rigid polymeric bilayers of **2** and phosphatidylcholine bilayers are forming an integrated composite membrane system, where the fluid phosphatidylcholine

(54) Groves, J. T.; Boxer, S. G.; McConnell, H. M. *Proc. Natl. Acad. Sci. U.S.A.* **1997**, *94*, 13390–13395.

bilayers are spatially confined by the micropatterned barriers of polymerized **2** bilayers.

#### 4. Conclusion

Photopolymerization of diacetylene amphiphiles **1** and **2** in SPB showed strong dependency on the underlying substrates. Most notably, a thin polymer layer covering the substrate surface could alter the polymerization process of the bilayers significantly. The observation that polymerization occurs also on polymeric materials, such as PEI and chitosan, is an important step toward the construction of polymer-supported patterned lipid membrane systems envisaged in Figure 1. The reconstitution of fluid bilayer membranes on polymeric support layers represents an important technical challenge to be addressed in the future studies.<sup>55</sup> The comparison between two types of diacetylene amphiphiles, the single chain alkyl phosphate **1** and the double chain phospholipid **2**, yielded insight into the importance of the type and nature of the polymerization process for the fabrication of two-dimensional micropatterned structures. The single chain diacetylene amphiphile **1** polymerized much more efficiently than the double chain counterpart, owing to its favorable molecular packing within the bilayer. However, at the same time it developed sharp domain structures with defects and made the polymerized film mechanically less stable. The double chain diacetylene phospholipid **2**, on the other hand, had a less favorable packing of molecules for the polymerization. It resulted in a slower polymerization and a shorter conjugation length. Nevertheless, the formed polymeric bilayers showed a much

higher stability. This is presumably due to the fact that each molecule has two polymerizable groups and the formed polymeric bilayer should contain some degree of cross-linking. Furthermore, the packing difficulties of the phospholipid seem to prevent the formation of sharp domain boundaries. These observations lead us to the realization that an amorphous, highly cross-linked network should be built within the polymerized bilayer, so that it can stabilize the whole membrane structure most effectively.<sup>56</sup> Our current study has demonstrated that patterned polymeric bilayers of **2** can act as a template to incorporate lipid bilayer membranes. The micropatterning strategy based on lithographic photopolymerization of lipid bilayers should provide new possibilities to construct complex and versatile biomimetic membrane systems by enhancing mechanical stability, creating spatial definition, and thus enabling the design of additional functions.

**Acknowledgment.** We thank Professor H. Ringsdorf (Johannes Gutenberg Universität, Mainz) for the kind gift of polymerizable monoalkyl phosphate **1**, Mr. B. Zimmer for his support in the fluorescence spectroscopy measurements, and Dr. H. Schönherr (University of Twente, The Netherlands) for critical reading and helpful comments on the manuscript. The work was supported by the Ministerium für Bildung, Wissenschaft, Forschung und Technologie (BMBF) (Project No. 0310852), the Schloesmann Foundation Fellowship (K.M.), and Graduierten Kolleg Stipendium (T.B.).

LA0157420

(55) Adsorption of SPB on PEI and chitosan polymer layers has been reported in previous studies (Wong, J. Y.; Majewski, J.; Seitz, M.; Park, C. K.; Israelachvili, J.; Smith, G. S. *Biophys. J.* **1999**, *77*, 1445–1457. Baumgart, T. Ph.D. Thesis, Johannes Gutenberg Universität, Mainz, 2001.) In the current study, however, we have not investigated the incorporation of fluid egg-PC bilayers into the micropatterned bilayers on polymeric supports.

(56) Considering the fact that diacetylene lipids are rather brittle crystalline materials, one could possibly achieve a better mechanical stabilization by employing less rigid polymerizable lipids. For example, some sorbyl-group-based lipid bilayers were recently demonstrated to polymerize on solid substrates. (Ross, E. E.; Bondurant, B.; Spratt, T.; Conboy, J. C.; O'Brien, D. F.; Saavedra, S. S. *Langmuir* **2001**, *17*, 2305–2307.) This could be regarded as one of the attractive candidates for the construction of patterned polymeric bilayers.